

## Fabry–Pérot resonators for surface plasmon polaritons probed by cathodoluminescence

M. Kuttge,<sup>a)</sup> E. J. R. Vesseur, and A. Polman

Center for Nanophotonics, FOM-Institute AMOLF, Sciencepark 113, 1098XG Amsterdam, The Netherlands

(Received 5 December 2008; accepted 8 April 2009; published online 4 May 2009)

Surface plasmon polariton Fabry–Pérot resonators were made in single-crystalline gold by focused ion beam milling of two parallel 100 nm deep grooves. The plasmonic cavity modes were spatially and spectrally resolved using cathodoluminescence spectroscopy. Mode numbers up to  $n=10$  were observed. The cavity quality factor  $Q$  depends strongly on groove depth; the highest  $Q=21$  was found for groove depth of 100 nm at  $\lambda=690$  nm. The data are consistent with finite-difference time domain calculations that show that the wavelength of maximum reflectivity is strongly correlated with groove depth. © 2009 American Institute of Physics. [DOI: 10.1063/1.3126484]

Surface plasmon polaritons (SPPs) are electromagnetic waves bound to the interface between a metal and a dielectric.<sup>1</sup> The strong coupling between optical radiation and the collective plasmon oscillations of the conduction electrons near the metal surface leads to large field enhancements at the interface. At frequencies close to the plasmon resonance, SPPs possess large wave vectors enabling sub-100 nm optics at optical frequencies. By varying the metal thickness, the SPP dispersion can be further tailored. SPPs thus enable two-dimensional optics in which optical information can be guided and processed at the nanoscale. While the propagation of SPPs has been well studied,<sup>2–5</sup> a next challenge is to obtain control over the confinement of SPPs.

So far, reflectors composed of arrays of nanoparticles<sup>6</sup> and Bragg cavities<sup>7</sup> composed of arrays of very shallow grooves or ridges have been studied to achieve SPP confinement. Weeber *et al.*<sup>7</sup> showed that two parallel ridge gratings can act as Bragg-mirrors and can confine plasmons between the mirrors. Because of the narrowband reflection of these gratings the field enhancement was only observed for a small wavelength range.

In this letter, we use a single deep groove in the surface of single crystalline gold as an effective mirror for surface plasmons. By placing two parallel grooves on the surface we construct a Fabry–Pérot resonator for SPPs. We use cathodoluminescence (CL) imaging spectroscopy<sup>3,4</sup> to excite the resonators and determine the spatially resolved cavity field profile. From the observed field profile we determine the mode numbers and cavity quality factor. Studies of the quality factor as a function of groove depth show a maximum of  $Q=15$  at a groove depth of 100 nm. Finite-difference time domain (FDTD) calculations of the groove reflectivity show an increase of reflectivity for these depths, supporting the experimental observations.

Experiments were performed on a single-crystal Au pellet of 1 mm thickness (effectively semi-infinite for optical fields) of which the surface was chemically polished down to nanometer roughness. Two parallel linear grooves were milled into the surface with a 30 keV Ga<sup>+</sup> focused ion beam [see schematic in Fig. 1(a)]. The groove separation  $w$  was 3000 nm, the depth  $d$  was 100 nm, and the groove width was 50 nm full width at half maximum (FWHM). The groove

shape and geometry were determined from scanning electron microscopy (SEM) images of a cross section of a groove pair [see Fig. 1(b)]. To fabricate the cross section a box was milled into the surface next to the grooves. To achieve the proper contrast to image the gold profile, platinum was first deposited over the grooves with focused-ion beam assisted deposition.

Spatially resolved CL spectroscopy was performed in a SEM using a 30 keV electron beam from a field-emission source focused onto the sample to a  $\sim 5$  nm diameter spot. The electron beam effectively acts as a point source for SPPs with a broadband spectrum ranging from the SPP resonance at 550 nm well into the infrared.<sup>3,4</sup> The scanning electron beam passes through a hole in a parabolic mirror that is positioned above the sample. The mirror collects light emitted from the sample, that is then focused on the entrance slit of a monochromator and spectrally resolved using a charge coupled device array detector (bandwidth  $\approx 10$  nm). The mirror acceptance solid angle is  $1.42\pi$ . The measured CL spectra were corrected for system response, which was determined by normalizing the measured raw data from a planar Au sample (no grooves) to the calculated transition radiation spectrum for 30 keV electron-irradiated Au.<sup>8</sup> The experimental count rate was 100–500 counts/s per wave-

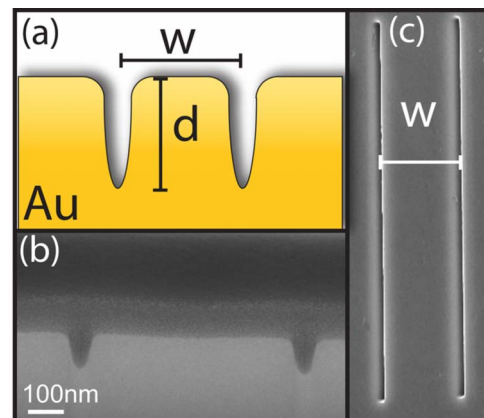


FIG. 1. (Color online) (a) Schematic of the double-groove Fabry–Pérot cavity in a gold surface. (b) Cross-section SEM image of the double groove structure. The grooves were filled with platinum and then a box was structured to allow side view. (c) SEM top-view of the double groove structure.  $w$  indicates the center-to-center groove spacing.

<sup>a)</sup>Electronic mail: kuttge@amolf.nl.

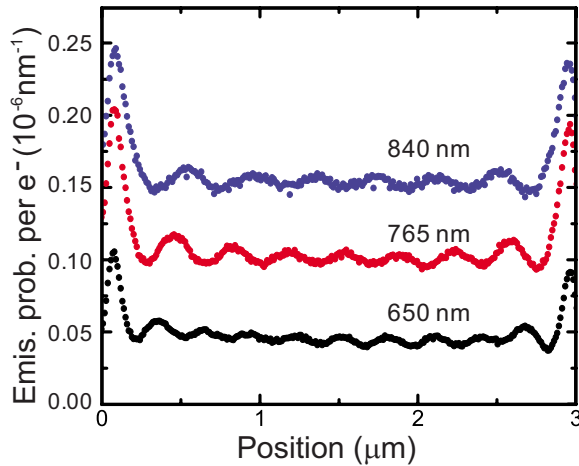


FIG. 2. (Color online) CL line scans (30 keV electron beam) over a double groove structure ( $w=3000$  nm and  $d=100$  nm) for wavelengths of 650 nm (black symbols), 765 nm (red symbols), and 840 nm (blue symbols). The grooves are located at 0 and 3  $\mu\text{m}$ . The curves are shifted by 0.05 (765 nm) and 1.0 (840 nm) for clarity.

length channel at an electron beam current of 28 nA.

We measured the CL spectra as a function of electron beam position along line scans perpendicular to the groove pairs with a step size of 5 nm and integration time of 1 s. Figure 2 shows the CL intensity for line scans over the double grooves for three different wavelengths (650, 765, and 840 nm). The peaks in the CL intensity coincide with the position of the grooves. Between the grooves a periodic pattern of the CL emission is observed for all wavelengths. The period of the oscillation equals approximately half the free-space wavelength for all three studied wavelengths.

The oscillations in the CL intensity are consistent with a standing SPP wave between the two grooves of the structure. The double-groove structure thus acts as a Fabry–Pérot resonator with the grooves acting as SPP reflectors. The interference condition for the SPP Fabry–Pérot cavity is given by  $2dk_{\text{SPP}} + 2\phi = 2\pi n$  with  $d$  the cavity length,  $k_{\text{SPP}}$  is the SPP wave vector,  $\phi$  is a phase shift upon reflection, and  $n$  is the mode number. Note that in CL spectroscopy the spatial resolution results from the known profile of the exciting electron beam. The oscillations in the radiation that are observed in the far field are due to the fact that the electron preferentially excites SPPs at positions of maximal electric field amplitude, i.e., the nodes in the standing wave pattern.

Figure 2 also shows that the visibility of the interference fringes increases with increasing wavelength. This is consistent with the larger SPP propagation length for larger wavelengths. For the shortest wavelengths the amplitude of the oscillations increases closer to the grooves again consistent with the shorter propagation length. Indeed, the SPP propagation length at 650 nm is a factor of 5 shorter than at 840 nm.<sup>5</sup>

To further study the Fabry–Pérot interference condition, we structured groove pairs with different groove separations into the gold surface, keeping the groove depth and width constant. Figure 3 shows the measured CL intensity as a function of position and wavelength for three groove separations of 1000, 2000, and 3000 nm, respectively. As can be seen, for wavelengths above 600 nm the measurements clearly show the standing wave pattern in the CL intensity. In the region below 600 nm the CL intensity decreases as a

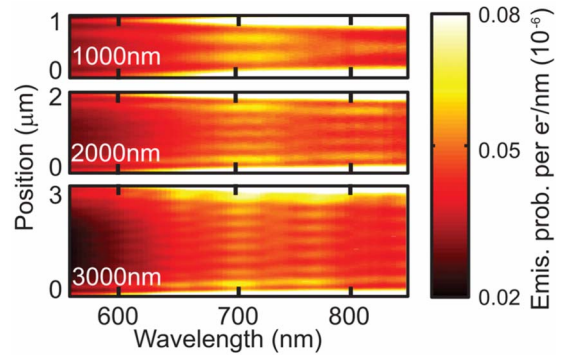


FIG. 3. (Color online) CL as a function of position and wavelength for line scans across three SPP Fabry–Pérot resonators with different center-to-center groove separation ( $w=1000$ , 2000, and 3000 nm). Multimode spectra with  $n=2-10$  are observed.

function of distance to the grooves showing only weak oscillations in particular for the largest cavity. In this region the SPP propagation length is shorter than the cavity length and no standing waves can form.

From the intensity maxima observed in Fig. 3 the resonant modes can be identified. For example, for the 1000 nm wide resonator two maxima are observed in the standing wave pattern at 700 nm, corresponding to a  $n=3$  mode. Similarly,  $n=6$  and  $n=9$  modes are observed at 700 nm for the 2000 and 3000 nm wide resonators. Due to the smaller free spectral range for the 3000 nm wide cavity a broad distribution of modes is observed around 700 nm ranging from  $n=7-11$ .

It is interesting to note that a  $n=3$  mode at 700 nm would correspond to a resonator width of 1020 nm (taking into account the dispersion of SPPs at 700 nm) which is 20 nm wider than the center-to-center spacing of the grooves. This implies that the effective cavity length is larger than the center-to-center spacing. This is consistent with the fact that the SPPs “probe” the depth of the grooves in their reflection. In this model the effective cavity length offset should be identical (20 nm) for all cavity lengths. Indeed, the  $n=6$  and  $n=9$  modes shift to slightly shorter wavelengths for the 2000 and 3000 nm resonators.

Next, we determined the quality factor of the resonators. To do so, we have structured a range of resonators into the single-crystal gold surface for which we varied the groove depth and thereby the reflectivity. The depth was varied in the range of 20–200 nm keeping the width approximately constant to 50 nm FWHM. The CL intensity was measured on a line perpendicular to the grooves with a step size of 10 nm. The CL line scans show interference fringes as in Fig. 2 for all wavelengths but with different degrees of visibility. The visibility increases with increasing depth for groove depths up to 100–120 nm. For deeper grooves the visibility decreases.

To determine the quality factors we performed a factor analysis<sup>9</sup> on the spectral CL line scan for a groove depth of 100 nm and width of 3000 nm (see Fig. 3) to determine the resonance spectra. Five significant resonances at wavelengths of 640 nm ( $n=10$ ), 690 nm ( $n=9$ ), 765 nm ( $n=8$ ), 870 nm ( $n=7$ ), and 980 nm ( $n=6$ ) were found to represent the data well. We reconstructed the experimental data from the resonances by fitting their line width and spatial position. The quality factor for each resonance is then given by the

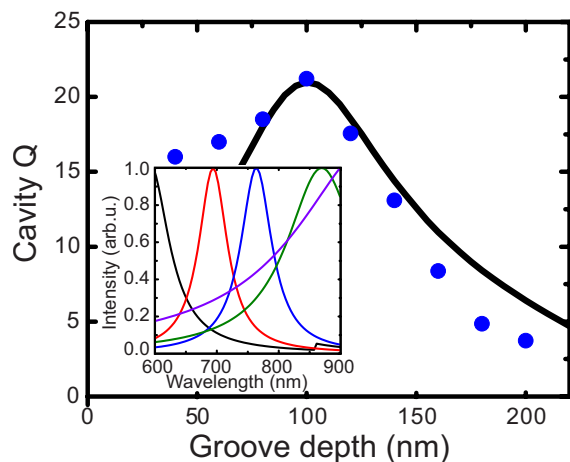


FIG. 4. (Color online) Quality factor for groove resonators for the resonance at 690 nm as a function of groove depth, extracted from CL line scans (symbols). The black line shows the quality factor calculated from the theoretical groove reflectivity and cavity losses. The inset shows the resonance spectra at 640, 690, 765, 870, and 980 nm derived from CL data for a resonator with 100 nm deep grooves ( $w=3000$  nm, last panel in Fig. 3).

resonance wavelength divided by the line width. The inset of Fig. 4 shows the five resonance spectra. The smallest line widths are observed for the central modes at 690 and 765 nm. Lower quality factors are observed for the 640 as well as the 870 and 890 nm modes.

The quality factor of the resonator is determined by propagation losses and the reflectivity of the mirrors. For the shortest wavelength (640 nm), propagation losses dominate, as was also apparent from Fig. 2 and a larger line width is observed (see inset of Fig. 4). To determine the reflectivity of a single groove for SPPs we have performed FDTD calculations. We used a two-dimensional simulation with the groove profile modeled according to the SEM images of the cross cuts. The SPP mode was generated at a distance of  $2 \mu\text{m}$  away from the groove. Reflection and transmission of the groove were monitored using field monitors past the groove and behind the source. Figure 5 shows the calculated groove reflectivity as a function of wavelength and groove depth. For each wavelength a maximum of the reflection coefficient is observed for a certain groove depth. The wavelength of the maximum increases with groove depth pointing to a reso-

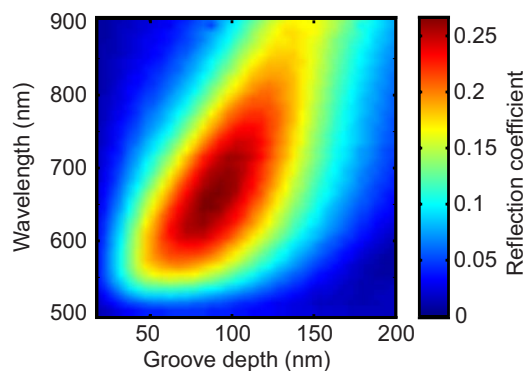


FIG. 5. (Color online) Reflection coefficient for SPPs at a single 100 nm wide groove in gold as a function of groove depth and SPP wavelength, as determined from FDTD calculations.

nance condition for the reflectivity maximum. Indeed, further calculations showed that the reflectivity is related to resonant localized modes inside the groove cavities.<sup>10</sup> The wavelength of the maximum increases with groove depth. The maximum reflection coefficient for 100 nm deep grooves is observed in the range of 650–700 nm. This is consistent with the smaller line width observed for the modes in that wavelength range in the inset of Fig. 4 or, correspondingly, the fact that the highest visibility resonances in Fig. 3 are observed around 700 nm. For wavelengths longer than 800 nm the reflectivity decreases as the incoming SPP is only slightly perturbed by the groove.

We have performed the factor analysis for the line scans of the other depths (20–200 nm). Figure 4 shows the quality factor for the resonance near 690 nm as a function of groove depth. The quality factor increases for increasing groove depth reaching a maximum of  $Q=21$  at 100 nm and decreases for larger groove depths. This is again consistent with Fig. 5.

Taking into account the reflectivity of the grooves and damping by the metal the theoretical quality factor can be calculated. In Fig. 4 we present the theoretical quality factor that shows a maximum of  $Q=21$  for 100 nm deep grooves in good agreements with experiments.

In conclusion, we have investigated Fabry–Pérot resonators for SPPs consisting of two parallel grooves. CL allowed direct imaging of the field profile inside the cavities and determine mode numbers up to  $n=10$ . The cavity quality factor was found to depend strongly on groove depth and wavelength, showing a maximum of  $Q=21$  at 700 nm for a groove depth of 100–120 nm. Further work will focus on achieving understanding of the details of the groove reflection of SPPs, taking into account localized modes inside the groove cavities.<sup>10</sup>

Harry Atwater and Henry Lezec are acknowledged for support in the previous stages of sample fabrication. This work is part of the research program of FOM, which is financially supported by NWO. This work is also supported by NANONED, a nanotechnology program funded by the Dutch Ministry of Economic Affairs, and the MMN research program which is partially financed by FEI Co.

<sup>1</sup>H. Raether, *Surface Plasmons on Smooth and Rough Surfaces and on Gratings* (Springer, New York, 1988).

<sup>2</sup>J. R. Krenn, H. Ditlbacher, G. Schider, A. Hohenau, A. Leitner, and F. R. Aussenegg, *J. Microsc.* **209**, 167 (2003).

<sup>3</sup>J. T. van Wijngaarden, E. Verhagen, A. Polman, C. E. Ross, H. J. Lezec, and H. A. Atwater, *Appl. Phys. Lett.* **88**, 221111 (2006).

<sup>4</sup>M. V. Bashevoy, F. Jonsson, A. V. Krasavin, N. I. Zheludev, Y. Chen, and M. I. Stockman, *Nano Lett.* **6**, 1113 (2006).

<sup>5</sup>M. Kuttge, E. J. R. Vesseur, J. Verhoeven, H. J. Lezec, H. A. Atwater, and A. Polman, *Appl. Phys. Lett.* **93**, 113110 (2008).

<sup>6</sup>A. Drezet, A. L. Stepanov, H. Ditlbacher, A. Hohenau, B. Steinberger, F. R. Aussenegg, A. Leitner, and J. R. Krenn, *Appl. Phys. Lett.* **86**, 074104 (2005).

<sup>7</sup>J.-C. Weeber, A. Bouhelier, G. Colas des Francs, L. Markey, and A. Dereux, *Nano Lett.* **7**, 1352 (2007).

<sup>8</sup>N. Yamamoto, H. Sugiyama, and A. Toda, *Proc. R. Soc. London, Ser. A* **452**, 2279 (1996).

<sup>9</sup>E. R. Malinowski, *Factor Analysis in Chemistry* (Wiley, New York, 1991).

<sup>10</sup>M. Kuttge, F. J. García de Abajo, and A. Polman, "How grooves reflect and confine surface plasmon polaritons," *Opt. Express* (submitted).